A laboratory model of splash-form tektites

Linda T. ELKINS-TANTON,[1, 2*] Pascale AUSSILLOUS,[3] José BICO,[4]
David QUÉRÉ,[3] and John W. M. BUSH[5]

[1]Department of Geological Sciences, Brown University, Providence, Rhode Island 02912, USA
[2]Department of Earth and Planetary Science, Massachusetts Institute of Technology, Cambridge, Massachusetts 02139, USA
[3]Laboratoire de Physique de la Matière Condensée, UMR 7125 du CNRS, Collège de France, 75231 Paris Cedex 05, France
[4]Department of Mechanical Engineering, Massachusetts Institute of Technology, Cambridge, Massachusetts 02139, USA
[5]Department of Mathematics, Massachusetts Institute of Technology, Cambridge, Massachusetts 02139, USA
[*]Corresponding author. E-mail: Linda_Elkins_Tanton@brown.edu

Abstract–Splash-form tektites are generally acknowledged to have the form of bodies of revolution. However, no detailed fluid dynamical investigation of their form and stability has yet been undertaken. Here, we review the dynamics and stability of spinning, translating fluid drops with a view to making inferences concerning the dynamic history of tektites. We conclude that, unless the differential speed between the molten tektite and ambient is substantially less than the terminal velocity, molten tektites can exist as equilibrium bodies of revolution only up to sizes of 3 mm. Larger tektites are necessarily non-equilibrium forms and so indicate the importance of cooling and solidification during flight. An examination of the shapes of rotating, translating drops indicates that rotating silicate drops in air will assume the shapes of bodies of rotation if their rotational speed is 1% or more of their translational speed. This requirement of only a very small rotational component explains why most splash-form tektites correspond to bodies of revolution. A laboratory model that consists of rolling or tumbling molten metallic drops reproduces all of the known forms of splash-form tektites, including spheres, oblate ellipsoids, dumbbells, teardrops, and tori. The laboratory also highlights important differences between rolling drops and tumbling drops in flight. For example, toroidal drops are much more stable in the former than in the latter situation.

INTRODUCTION

Tektites, glassy or crystalline bodies ranging in size from micrometers to 0.1 m, are ejecta from terrestrial impact craters (e.g., Taylor 1973; King 1977; Barnes 1990; Koeberl 1990). The majority of papers on tektites have been dedicated to determining the source of tektites or to attempting to discover the terrestrial crater from which they were ejected. While splash-form tektites are generally acknowledged to have the form of bodies of revolution, a detailed fluid dynamical investigation of their form and stability has not been undertaken. Here, we clarify why tektites correspond to bodies of revolution and present a simple new laboratory model that allows for the generation of synthetic tektite forms.

Tektites can be divided by structure and shape into 4 categories: Muong Nong, or layered tektites; microtektites, glassy or crystalline bodies less than a mm in diameter; splash-form tektites, including spheres, ellipsoids, tori, and dumbbells; and ablated tektites. Reinhart (1958) coined the term "splash-form," hypothesizing that such tektites are formed by melt splashed by impacts and that their size is controlled by surface tension. Subsequently, most researchers have described these tektites as "bodies of rotation" (e.g., Barnes and Barnes 1973). Ablated tektites are splash-form tektites that were partially remelted during atmospheric re-entry, during which their leading face is heated and melted by friction and the melt ablated, forming a rear-facing cusp around the perimeter of the tektite (Adams and Huffaker 1962, 1964). O'Keefe (1976) demonstrated that forms reminiscent of ablated tektites may be generated experimentally in a supersonic wind tunnel, where melting results from intense viscous dissipation in the boundary layer on the body. To date, this represents the only lab analogue for tektite formation; splash-form tektites have yet to be produced experimentally.

The largest splash-form tektite on record is a 1069 g piece from the Philippines (Walcott 1898; Beyer 1962; Barnes and Barnes 1973; O'Keefe 1976). Spherical tektites have been found with diameters ranging from 50 μm to at least 5 cm, a

range of 3 orders of magnitude (O'Keefe 1976). Dumbbells have been found with lengths from 10 μm (Stanley et al. 1971) to at least 15 cm (O'Keefe 1976), and ellipsoids come in a similar size range. While toroidal tektites are more rare, McColl (1997) reports an ablated toroidal form with a radius of 2 cm.

We assume that tektites are produced by terrestrial impacts either directly from the splashing of shock melt or, possibly, as condensates from the vapor cloud created by the impact (e.g., Margolis et al. 1991). In the latter case, coalescence of tektite fluid during descent is expected to give rise to tektite rain or hail (Melosh 1990). Note that tektites containing lechatelierite or other source remnants cannot have condensed from a vapor, and tektites with compositions closely allied to their sources are also not likely to be condensates. In either case, the final product is a fluid drop in flight; this physical system will be our subject of focus. If tektites are indeed produced by the splashing of shock melt, one expects a minimum size to be prescribed by the dynamics of their breakup. Moreover, a maximum size exists for equilibrium fluid bodies of revolution bound by surface tension. Thus, we summarize existing literature on the stability of translating, rotating fluid drops to make inferences concerning the dynamic history of tektites based on their observed size range.

Clift et al. (1978) characterize the shapes of liquid drops of density (ρ), dynamic viscosity (η), and volume (V) = $4\pi R^3/3$, translating through an ambient with density (ρ_a) with relative velocity (ΔU). The drops are assumed to have a constant surface tension (σ). This system is uniquely prescribed in terms of 2 dimensionless groups, specifically, the drop Reynolds (Re) and Weber numbers (We), defined as follows:

$$Re = \frac{\rho R \Delta U}{\eta}, We = \frac{\rho_a R \Delta U^2}{\sigma} \qquad (1)$$

High Re drops in pure translation are axisymmetric about the direction of motion, and asymmetric forms arise from wobbling drop motions. The breakup of a mass of fluid will, in general, result in the generation of irregular fluid bodies that tumble under the influence of aerodynamic torques. Tumbling fluid drops are, thus, a natural byproduct of the fracture of a fluid mass in flight.

We consider the dynamics of spinning drops translating through air. First, we consider the case of an isothermal drop with material properties that are constant. In the section The Scale and Stability of Flying Drops, we describe the scaling governing the dynamics, form and stability of rotating, translating drops. In the Experiments section, we detail the experimental study in which we reproduce all known shapes of splash-form tektites. A brief discussion of the thermodynamic considerations required for the more complex case of cooling drops, the material properties of which necessarily change with time, is presented in the Discussion section.

THE SCALE AND STABILITY OF FLYING DROPS

We proceed by summarizing the dynamics and stability of tumbling fluid drops, considering, in turn, the influence of translation and rotation.

Drops in Translation

The simplest relevant problem of fluid stability involves a fluid drop falling under the influence of gravity. A fluid volume of density (ρ) and characteristic scale (R) falling under the influence of gravity (g) will accelerate until its weight is balanced by the aerodynamic drag. Assuming that the drop motion is characterized by a high Reynolds number (Re), this balance may be expressed:

$$\rho_a U^2 R^2 \approx \rho R^3 g \qquad (2)$$

where $\rho_a << \rho$ denotes the density of air. The drop then achieves its terminal speed:

$$U \approx \left(\frac{\rho}{\rho_a} g R\right)^{1/2} \qquad (3)$$

If the fluid volume is sufficiently large, it will breakup, giving rise to a series of drops (Hsiang and Faeth 1992). The cascade to smaller drops will continue until the curvature force associated with the drop surface tension is sufficient to balance the dynamic pressures associated with the drop translation:

$$\rho_a U^2 \approx \frac{\sigma}{R} \qquad (4)$$

Substitution for the terminal speed (U) indicates that the maximum drop size achieved will be the capillary length:

$$R_c \approx \left(\frac{\sigma}{\rho g}\right)^{1/2} \qquad (5)$$

The capillary length for an air-water system (σ = 0.07 N/m, ρ = 1000 kg/m^3) prescribes the maximum size of raindrops: R_c ~0.003 m. Characteristic surface tensions and densities for liquid silicates (see Table 1) indicate that terminal velocities for tektite fluid are on the order of 30 m/s and that the capillary length is not changed substantially for tektites.

In the absence of cooling, one expects that fluid falling solely under the influence of gravity will result in drops comparable in size to raindrops. More generally, a drop subject to an acceleration (a) will have a size scaling as R_c, with (g) replaced by (a) in Equation 5. The further effects of rotation and viscosity are discussed below.

Droplet Breakup

If a fluid mass is initially propelled relative to the ambient at a speed (ΔU) that exceeds its terminal speed, drops

Table 1. Non-dimensional numbers for experiments and natural tektites.

Physical parameters	Exp. 1 Fig. 4	Exp. 2 Fig. 5	Exp. 3 Fig. 7	Exp. 4 Fig. 8	Tektite min. (approx.)	Tektite max. (approx.)	Units
ρ, fluid density	7130	7130	7130	1260	2700	3200	kg/m^3
R, fluid length scale	0.0015	0.003	0.0035	0.0035	10^{-4}	0.05	m
R$_o$, fluid length scale (radius of equivalent sphere)	0.0007	0.0014	0.0021	0.0019	–	–	m
σ, surface tension	0.53	0.53	0.53	0.06	0.2	0.5[a]	N/m
η, fluid viscosity	0.5	0.5	0.5	1.2	0.1	1000[b]	Pa s
ΔU, relative speed	0.6	0.8	0.7	2.5	1	100[c]	m/s
Ω, rotational velocity	310	260	190	107	1	5000	rad/s
Non-dimensional numbers							
Bond number	0.06	0.33	0.56	0.21	10^{-9}	10^6	
Weber number	0.0005	0.0017	0.0019	0.20	10^{-4}	10^3	
Ohnesorge number	0.2	0.2	0.1	2.2	10^{-2}	10^3	
We$_{critical}$	13	13	12	59	10	10^6	
Sigma	960	1524	2304	8	10^{-5}	10^4	
ΩR	0.2	0.4	0.4	0.2	10^{-4}	10^2	
0.01 ΔU	0.006	0.008	0.007	0.025	10^{-2}	1	
R$_{crit}$, maximum size	0.0015	0.0017	0.0021	0.0027	3×10^{-4}	8×10^{-2}	

[a]Silicate surface tension values from Riley and Kohlstedt (1991).
[b]As described in the text, tektite fluid can be as viscous as 10^{13} Pa s.
[c]This is the range of relative velocities used in calculations and based on the computations of Stöffler et al. (2002); a more conservative estimate would extend the upper bound to the velocity of impact, on the order of 10^4 m/s.

smaller than R$_c$ may result. Specifically, one expects the fluid mass to breakup until the resulting drops are sufficiently small to be stabilized by surface tension:

$$\rho_a \Delta U^2 \approx \frac{\sigma}{R} \qquad (6)$$

that is, until they achieve a size characterized by a breakup length:

$$R_b \approx \frac{\sigma}{\rho_a \Delta U^2} \qquad (7)$$

If the relative drop speed is assumed to be comparable to the characteristic impact speeds (estimated at U$_i$ ~10 to 70 km/s; Steel 1998), one expects tektite breakup to result in droplets as small as 1 µm. However, generally, a high-speed radial efflux of gas occurrs following the impact; consequently, one expects ΔU << U$_i$ (Melosh and Vickery 1991), resulting in the possibility of larger tektites. The numerical models of Stöffler et al. (2002) indicate relative velocities (ΔU) on the order of 1–100 m/sec; these values will be adopted in our calculations and would suggest tektite sizes in the range of 10 µm–10 cm, in the absence of rotation (see Table 1).

Pilch and Erdman (1987) present the results of an experimental study of the breakup of liquid droplets in flight. Specifically, they detail the dependence of the precise form of droplet breakup on the Weber number (We) (see Equation 1). A droplet will breakup via pinch-off or by a range of more violent mechanisms, according to its Weber number. In general, a cascade of breakup events occurs until the resulting

drops achieve a stable size. The critical Weber number, below which drops are stable, depends on the Ohnesorge number (On):

$$On = \frac{\eta}{(2\rho R\sigma)^{1/2}} \qquad (8)$$

where η is the dynamic viscosity of the fluid. The Ohnesorge number prescribes the relative magnitudes of the characteristic time for pinch-off when viscosity dominates, ηR/σ, and the characteristic time for inertial breakup, (ρR^3/σ)$^{0.5}$ (Eggers 1997). We note that when tektites cool and become more viscous, the Ohnesorge number increases, as does the critical Weber number; droplet breakup is, thus, resisted. Thus, both capillary and viscous forces oppose the breakup of drops in flight. The empirical relation of Brodkey (1969), given here, is found to be adequate for On <30:

$$We_{crit} = 12(1 + 1.077On^{1.6}) \qquad (9)$$

The breakup process is enhanced by the high ejection speeds and low viscosities of molten silicates and retarded by cooling and quenching of the tektite fluid into a glass. The latter process necessarily increases the fluid viscosity, thus, increasing the breakup time and contributing to the drop stability. The strong temperature dependence of viscosity will, thus, have a significant influence on the ultimate size of the tektites. In particular, the cooling of the drops in flight will dramatically increase their viscosity and, therefore, resist the cascade to smaller scales.

The Influence of Rotation

Consider a fluid drop of density (ρ), volume $(V) = (4\pi R^3)/3$, and kinematic viscosity (ν) (where dynamic viscosity $[\eta] = \nu\rho$) translating in air (density $[\rho_a]$ and kinematic viscosity $[\nu_a]$) at a speed (ΔU) relative to ambient, while rotating with angular speed (Ω) and bound by a surface tension (σ). The drop dynamics are prescribed by the following dimensionless groups: the viscosity and density ratios, ν/ν_a and ρ/ρ_a; the Reynolds number, $Re = \Delta UR/\nu_a$; the Weber number, $We = \rho_a\Delta U^2R/\sigma$; and the ratio of the rotational and translational speeds, $\Omega R/\Delta U$. The relative magnitudes of the dynamic pressures generated by the drop rotation and translation for high Re drops is prescribed by:

$$\Sigma = \frac{\Delta\rho\Omega^2R^2}{\rho_a\Delta U^2} \qquad (10)$$

If $\Sigma \gg 1$, that is, $\Omega R \gg \Delta U(\rho_a/\Delta\rho)^{1/2}$, the dynamic pressures associated with the translation will have a negligible influence on the drop shape. Using characteristic values for the tektite density from Table 1 indicates that this limit is achieved provided:

$$\Omega R \gg 0.01\Delta U \qquad (11)$$

Therefore, tektites are expected to assume the form of bodies of rotation provided their rotational speed exceeds 1% of their translational speed. The fact that most tektites take the form of bodies of revolution thus follows from the large density difference between the tektite and the surrounding air.

Fluid drop shape is uniquely prescribed by the normal force balance at its surface. Provided the rotational and translation speeds are comparable, the balance is between centrifugal and curvature forces:

$$\Delta P + 4B_o\left(\frac{r}{R}\right)^2 = \nabla \cdot \hat{n} \qquad (12)$$

where the local surface is a distance (r) from the axis of rotation and has a unit normal (n). The rotational Bond number is defined by:

$$B_o = \frac{\rho\Omega^2R^3}{8\sigma} \qquad (13)$$

and $\Delta P = R\Delta\rho/\sigma$ is the dimensionless pressure difference between the drop center and the ambient.

The progression of drop shapes with B_o has been well documented (Chandrasekhar 1965; Brown and Scriven 1980). As B_o increases progressively from zero, the equilibrium drop shape evolves from a sphere to an oblate ellipsoid and then to a biconcave form. Chandrasekhar showed that at $B_o = 0.57$, axisymmetric drops no longer enclose the origin but, instead, assume a toroidal form. Figure 1 shows the theoretical predictions for the shapes of

axisymmetric rotating drops predicted by numerical integration of the force balance (Equation 12). Brown and Scriven (1980) considered the possibility of non-axisymmetric forms and demonstrated that lobed forms are possible. For $0.09 < B_o < 0.31$, Brown and Scriven (1980) demonstrated that there are 2 stable equilibrium forms, one an axisymmetric oblate ellipsoid and the other a 2-lobed (dumbbell or peanut) form. Solutions consisting of multi- (3- and 4-) lobed structures were also found to exist but to be unstable. For $B_o > 0.31$, axisymmetric shapes were found to be unstable, so one expects dumbbell forms to obtain.

Figure 2 illustrates the dependence of the shape of rotating fluid bodies bound by surface tension on the rotational Bond number (B_o) (Brown and Scriven 1980). The lower solid line denotes the family of stable oblate ellipsoids, and the upper line denotes the stable dumbbell shapes. The unstable family for $B_o > 0.31$ corresponds to biconcave ellipsoids, the precursor to toroidal shapes. Beyond $B_o = 0.57$, no equilibrium form exists, and the drop necessarily breaks into smaller drops. This yields a simple criterion for drop breakup induced by rotation:

$$\Omega R > 2.13\left(\frac{\sigma}{\rho R}\right)^{1/2} \qquad (14)$$

One, thus, infers that stable bodies of revolution may only exist up to a critical size prescribed by:

$$R_c = 1.66\left(\frac{\sigma}{\rho\Omega^2}\right)^{1/3} \qquad (15)$$

Using surface tension and density values appropriate for tektite fluid (see Table 1) indicates susceptibility to breakup if the rotational speed (ΩR) exceeds 0.5 m/s, which is considerably less than the translational speeds, even for a drop in free fall. Assuming that the rotational and translational speeds are comparable $\Delta U \sim \Omega R$ would suggest a maximum size:

$$R_c = 4.58\frac{\sigma}{\rho(\Delta U)^2} \qquad (16)$$

Setting ΔU to be the terminal speed (Equation 3), thus, yields the upper bound on the size of fluid equilibrium bodies of revolution: 3 mm. Tektites that are larger than the critical sizes defined by Equation 15 and 16 are necessarily non-equilibrium forms that cooled and solidified before breakup could arise. Alternatively, they may indicate anomalously low differential speeds between the fluid tektite and ambient before solidification; at arbitrarily low differential velocity and zero rotation, the tektite radius can approach 8 cm. We also note that the natural tektites shown in Fig. 2 are not necessarily equilibrium bodies of revolution but may be, rather, non-equilibrium shapes frozen into place during solidification. For example, tektite (c) assumes a metastable
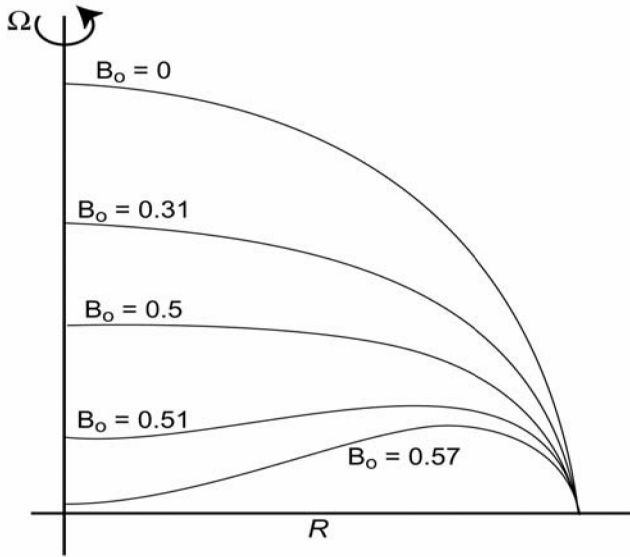
Fig. 1. The dependence of the shapes of axisymmetric fluid bodies of revolution bound by surface tension on the rotational Bond number $B_o = \rho\Omega^2 R^3/(8\sigma)$, as deduced from numerical integration of Equation 12. The figure represents the shape of the fluid body taken as a cross-section through the body. The rotation axis corresponds to the vertical axis; only the upper right quadrant is shown. Drop shapes for B_o <0.31 are unstable. All lengths are non-dimensionalized by the maximum (equatorial) radius.

Fig. 2. The ratio of the maximum radius to the unperturbed radius is indicated as a function of the rotational Bond number $B_o = \rho\Omega^2 R^3/(8\sigma)$. (Figure after Brown and Scriven [1980].) Stable parameters are denoted by the solid line, and metastable extensions by dashed lines. Predicted 3-dimensional forms are compared to photographs of natural tektites. As B_o increases progressively from 0, the equilibrium drop shape evolves from a sphere to an oblate ellipsoid. At $B_o = 0.5$, axisymmetric drops assume a toroidal form. For $0.09 <B_o <0.31$, 2 stable equilibrium forms exist: the axisymmetric oblate ellipsoid and the dumbbell. For B_o >0.31, no stable axisymmetric shape exists. For B_o >0.57, the non-equilibrium form exists, and the drop necessarily breaks into smaller drops. Natural splash-form tektites that lie outside the stability parameters shown here are the result of solidification before breakup. Tektite photos 2a, 2e, 2f, and 2g are from Baker (1963), 2b and 2d are from Cohen (1963), and 2c is from Norm Lehrman (www.TektiteSource.com). All scale bars are 1 cm.

biconcave form with a diameter of 15 cm that greatly exceeds the capillary length. Tektite (g) is also an obvious non-equilibrium size.

Tektites typically assume the forms of bodies of revolution, specifically spheres, ellipsoids, dumbbells, and even tori. Such fluid forms were first explored experimentally by Plateau (1863) owing to his interest in the form of heavenly bodies. A recent study by Aussillous and Quéré (2001) made clear that bodies of revolution may also arise when drops roll down a solid incline. That these should be bodies of revolution follows directly from our previous discussion, since, in this setting, the ratio of the drop and suspending fluid densities is large, while the rotational and translational speeds are necessarily comparable. We proceed by describing an experimental investigation in which model tektites are generated from rolling metal drops.

EXPERIMENTS

We focus on the laboratory analogues of splash-form tektites but also briefly discuss the non-tektite forms observed.

Apparati

Laboratory experiments were conducted in parallel in 2 laboratories, at the Laboratoire de Physique de Matière Condensée at the Collège d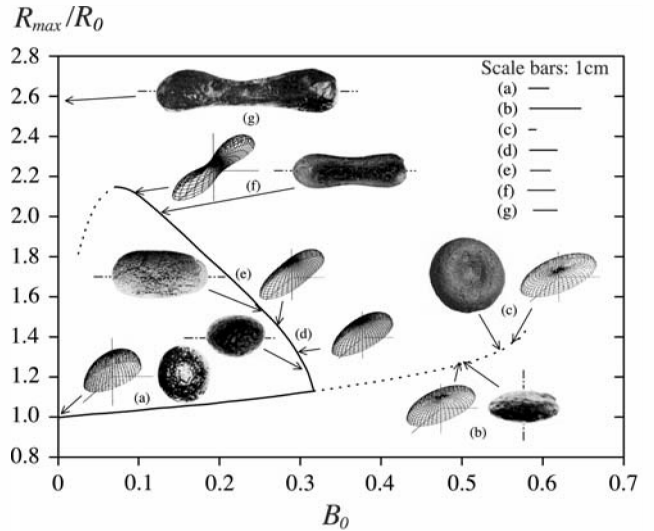e France and the Fluid Dynamics Laboratory in the Department of Mathematics at the Massachusetts Institute of Technology. The laboratory models of tektite formation were developed by adapting the experimental technique of Aussillous and Quéré (2001) who demonstrated that bodies of revolution arise naturally when viscous drops with a hydrophobic coating roll down an incline. Similar rotational motion was observed for viscous drops running on a super-hydrophobic substrate (Richard and Quéré 1999), in agreement with the theoretical predictions of Mahadevan and Pomeau (1999) for the non-wetting situation.

Three distinct experimental configurations were considered. The first configuration involved rolling molten solder drops down a planar incline and into a quenching bath in which the drops were quickly cooled and solidified. In the second configuration, the drops rolled off the end of the ramp, tumbling freely through the air. In the third configuration, drops were placed inside a cylindrical drum rotating about its horizontal axis at a rate prescribed by a DC-motor (Fig. 3). The annulus had a slight groove along its centerline that prevented the drops from rolling out of the cylinder. Two drums were used: one of aluminum, which allowed for the possibility of maintaining the drops in their molten state through heating the
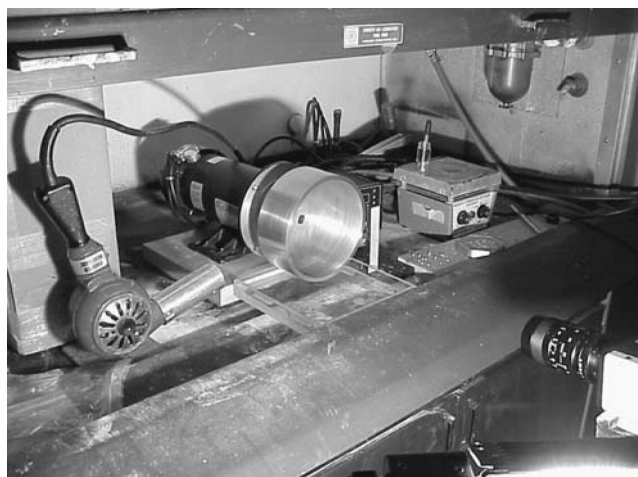
Fig. 3. Experimental apparatus used in the production of laboratory tektites. A cylindrical drum with a groove along its centerline is driven by a variable speed DC-motor. Both Celeron and aluminum drums were used.

drum with a jet of hot air; and one of Celeron, a mixture of wood and glass fiber, and an excellent insulator, with which we were able to trace the progression of cooling, solidifying molten metal drops. Drops were emplaced on the inner surface of the annulus, and the motor speed was adjusted to match the drop rolling speed so that quasi-steady states could be attained. Two types of metallic drops were examined. The first was the solder Cerrobend (50 wt% bismuth, 26.7 wt% lead, 13.3 wt% tin and 10 wt% cadmium; surface tension [σ] = 0.38 N/m, density [ρ] = 9700 kg/m^3), which has a melting point of 70°C and was easily maintained in its liquid state. The second was pure tin (σ = 0.53 N/m, ρ = 7130 kg/m^3), which has a melting temperature of 233°C and solidified in the laboratory atmosphere. The high surface tension of the molten metals ensures that the drops are in a situation of non-wetting, which suppresses the adhesion properties and dissipation processes associated with the presence of contact lines.

Tektite Forms

Analogue laboratory tektites were generated from both rolling and tumbling metallic droplets. When the drop volume was sufficiently small (on the order of 0.05 cm^3), the drop rolled down the incline without significant distortion due to contact forces and assumed the forms of bodies of revolution, specifically oblate ellipsoids, dumbbells, and tori. A time-sequence of a tektite form rolling along an incline is illustrated in Fig. 4. Tumbling forms were observed by letting the drops roll off the edge of a ramp and tumble through the air. A dumbbell-shaped lab tektite tumbling along a parabolic trajectory is illustrated in Fig. 5.

Photographs of several synthetic model tektites produced in our experiments are presented in Fig. 6. We note that all of the laboratory tektites so generated were on the scale of

Fig. 4. High-speed camera images of a synthetic tin "tektite" tumbling along a ramp. Images are taken at a time interval of 8 ms. The reference scale at top left is 1 cm. This experiment is labeled "1" in Fig. 10.
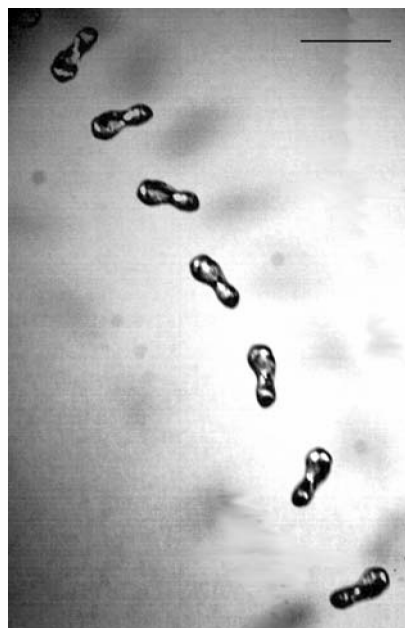

Fig. 5. High-speed camera images of a dumbbell-shaped synthetic laboratory "tektite" tumbling through the air after leaving a ramp. The synthetic tektite material is tin. Images are taken at a time interval of 10 ms. The reference scale is 1 cm. This experiment is labeled "2" in Fig. 10.

millimeters. The largest forms were clearly influenced by interaction with the lower boundary and will be discussed as non-tektite forms in the next section. The smaller forms, specifically the dumbbells (Fig. 6a) and small discs (Fig. 6b), are largely uninfluenced by the lower boundary. Non-equilibrium teardrop forms were observed to arise from the breakup of dumbbell shapes. A time sequence illustrating the breakup of a rolling disc and the resulting emergence of a tear-dropped shape is presented in Fig. 7. Note that the teardrop's tip, a transient state in drop fracture, is made permanent by solidification, the influence of which is particularly efficient in the tip region where the surface area to volume ratio is high.

Non-Tektite Forms

When the drop volumes were sufficiently large (greater than 1 ml), their forms were significantly influenced by their interaction with the lower boundary. The largest structures resembled flattened circular puddles that advanced through a
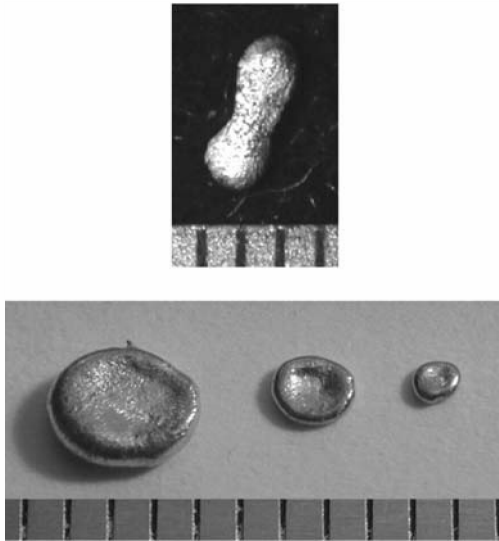
Fig. 6. Synthetic tektite forms produced in our laboratory study from rolling Cerrobend solder drops: a) a dumbbell; b) oblate ellipsoidal and biconcave forms.
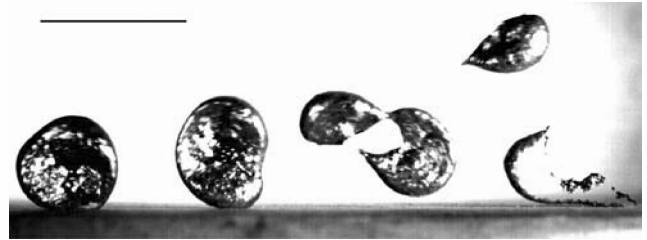

Fig. 7. Sequence illustrating the fracture of a rolling biconcave form into a teardrop. The synthetic tektite material is tin. The scale bar is 1 cm. The images are taken at intervals of 16 ms, and the slope is 30°. This experiment is labeled "3" in Fig. 10.
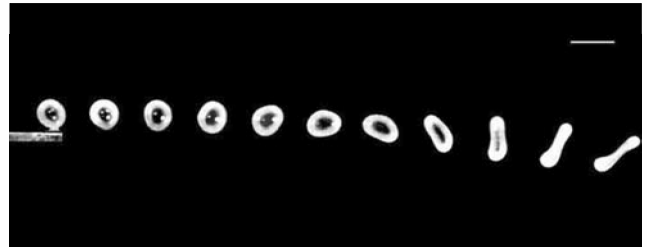

Fig. 8. High-speed camera images of a toroidal glycerol-water drop coated with a hydrophobic powder rolling off a ramp and transforming into a dumbbell as it tumbles. As soon as an axisymmetric drop leaves the substrate, it irreversibly transforms into the more stable dumbbell form. Images are taken at intervals of 5 ms, and the reference length scale is 1 cm. This experiment is labeled "4" in Fig. 10.

tractor-tread motion along the laboratory track. As the fluid volume was decreased, the puddles became elongated in the direction of motion so that the drop resembled a sausage, again advancing with a tractor tread motion. Further decreasing the drop volume lead to the tektite forms detailed in the previous section. Although disks and biconcave drops are not stable bodies of revolution (see Figs. 1 and 2), these were commonly obtained in the laboratory for solidifying rolling metal drops: the presence of the lower boundary evidently stabilizes these forms. The disc-shaped bodies have flattened edges resulting from their interaction with the lower surface.

To eliminate the influence of solidification, we used glycerol-water drops coated with a lycopodium powder, which makes them non-wetting, whatever the substrate. The influence of the lower boundary was eliminated by allowing the droplets to roll off the end of a ramp and tumble through the air. In the drum, we could, thus, observe either dumbbell or toroidal shapes. Figure 8 illustrates an initially toroidal water drop rolling off the end of the ramp and tumbling through the air in dumbbell form. The transformation occurs at a constant speed of rotation and typically takes 20 ms. We note that it is not necessary to remove the solid substrate as in Fig. 8 to observe such a transformation. The doughnuts are soft and can exhibit a slight eccentricity because of their weight: such an ellipsoidal body, when rolling on a solid, can spontaneously take off due to the motion of its center of mass. The transformation into a dumbbell is found to be irreversible, in accordance with the predictions of Brown and Scriven (1980). The existence of biconcave tektites may be related to the solidification process, which fixes this metastable shape before it evolves into the more stable dumbbell shapes.

Our experimental study, thus, made clear an important difference in the stability of rolling and freely tumbling drops. Specifically, toroidal forms are significantly more stable when rolling than tumbling: the transition from rolling to tumbling was accompanied by the axisymmetric toroidal forms being replaced by the dumbbell forms. This evolution is plainly evident in Fig. 8.

Finally, we considered the long-term evolution of cooling, rolling drops on a treadmill. By using the insulating Celeron track at room temperature, we are able to examine the progression of initially molten tin drops as they cool and solidify (Fig. 9). Initially, the drop is not sufficiently viscous to be in solid body rotation and takes the form of a flattened puddle that glides along the drum (Fig. 9a). Then, as the drop cools and its viscosity increases, it begins to rotate, a transition marked by the dramatic evolution of its shape, into disc then biconcave forms. Mahadevan and Pomeau (1999) suggest that the criterion for the onset of rotational motion is that the Reynolds number, Re (see Equation 1), be on the order of unity or larger. For a centimetric drop of molten metal descending at 0.5 m/s, this criterion requires a viscosity of about 10 Pa s. In the particular case of Fig. 9, the drop was sufficiently large to solidify slowly, which made the appearance of a hole at the drop center and collapse of the resulting form under the influence of gravity possible.
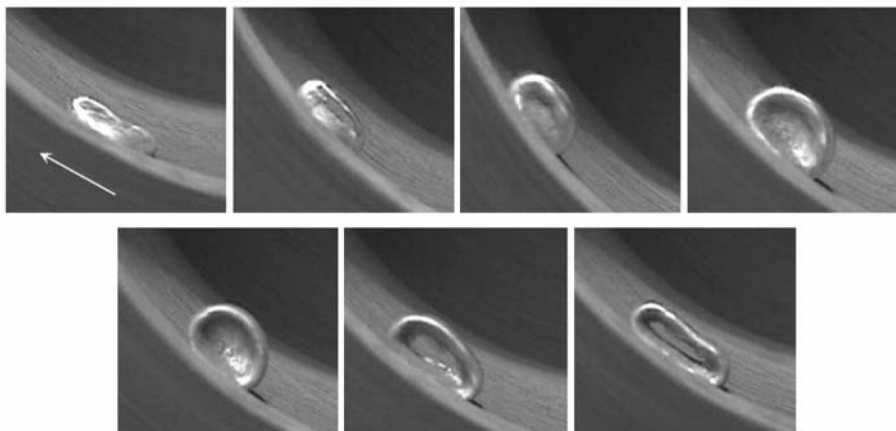
Fig. 9. Sequence illustrating a tin drop rolling and cooling on the Celeron track. As the drop cools, it begins to roll, assuming a biconcave form; subsequently, it collapses under the influence of gravity.

DISCUSSION

The physical parameters relevant to the dynamics of tektites in flight are listed in Table 1 along with appropriate non-dimensional numbers. For each of the 4 experiments shown in Figs. 4, 5, 7, and 8, the corresponding physical parameters and non-dimensional values are listed. The non-dimensional numbers describing the experiments fall within the range of natural tektites in each case.

Tektites will cool as they fall, and the strong dependence of silicate viscosity on temperature will inhibit breakup by the formation of a cold crust (O'Keefe 1976). Silicate viscosity is also highly dependent on the composition of the liquid: oxides that form networks, such as silica and alumina, increase viscosity, while non-bonding oxides, such as magnesium and sodium, reduce viscosity (Bottinga and Weill 1972). The models of Stöffler et al. (2002) indicate that, for the impact that created the Moldavite tektite strewn field, tektites were heated to as much as 3200°C and that, to a first approximation, material stayed above its liquidus for about 30 sec. Larger impacts may be expected to heat tektite material further. Melosh (1998) states that silicates at the site of impact will reach instantaneous temperatures of 50,000°C, remaining at 5,000 to 10,000°C for tens of seconds. We note that these temperatures are above many oxides' vaporization temperatures (e.g., Palme and Larimer 1988).

Applying the viscosity calculation techniques of Bottinga and Weill (1972) and Shaw (1972) to various tektite compositions (Glass 1972; Frey 1977; Meisel et al. 1997; Albin et al. 2000) suggests that, at their liquidus temperatures, tektites vary in viscosity from 10^2 to 10^7 Pa s. These results are in agreement with the calculations of Klein et al. (1980), who found tektite viscosities in the range 10^2 to 10^{13} Pa s over the temperature range of 700 to 1400°C. To investigate the influence of temperature on viscosity, we consider experimental and analytical results for magmatic liquids: Dingwell et al. (2000) found that granitic melts, some of which are reasonable analogues for tektites, vary in viscosity from 10^{10} to 10^{12} Pa s at 1000°C and from 1 to 10^3 Pa s at 2000°C. At 5000°C, Shaw (1972) estimates that most silicate liquids have a viscosity of about 0.1 Pa s and that the viscosity of basaltic liquids rises to only about 50 Pa s as they cool to their liquidus temperature. We, therefore, consider molten tektite viscosities in the range of 0.1 Pa s to 10^3 Pa s, as indicated in Table 1.

The limits on equilibrium length scales for natural tektites are shown in Fig. 10. The critical Weber number is shown as a function of the tektite length scale (R) in Fig. 10a for a range of velocities (ΔU). The critical Weber number, below which breakup does not occur, is shown as a function of viscosity. At R <0.001 m or ΔU <~30 m/s, tektites will not breakup from the dynamic pressures induced by their translation. Viscosity also opposes breakup: viscosities as low as 100 Pa s allow tektites as large as 0.05 m to exist even at ΔU >100 m/sec. Droplets with low viscosity (1 Pa s and less) and radii on the order of centimeters will breakup to cm- to mm-sized droplets, and at very high ΔU, they may breakup to droplets on the scale of tens to hundreds of μm. Thus, centimetric tektites may be stable, if their relative velocities are low, when they are not rotating. The effect of rotation is shown by the vertical lines in Fig. 10a: a cm-sized tektite is unstable if it is rotating even as slowly as 50 rad/s. Destabilization by rotation is demonstrated further in Fig. 10b. Only the smallest or most slowly rotating tektites can avoid breakup by rotation.

CONCLUSIONS

We have presented the results of a laboratory study of rolling or tumbling molten metal droplets. We have, thus, produced laboratory analogues of all known splash-form tektites, including spheres, oblate and prolate ellipsoids, tear drops, tori, and dumbbells. Our study also underlines a fundamental difference in the stability characteristics of rolling
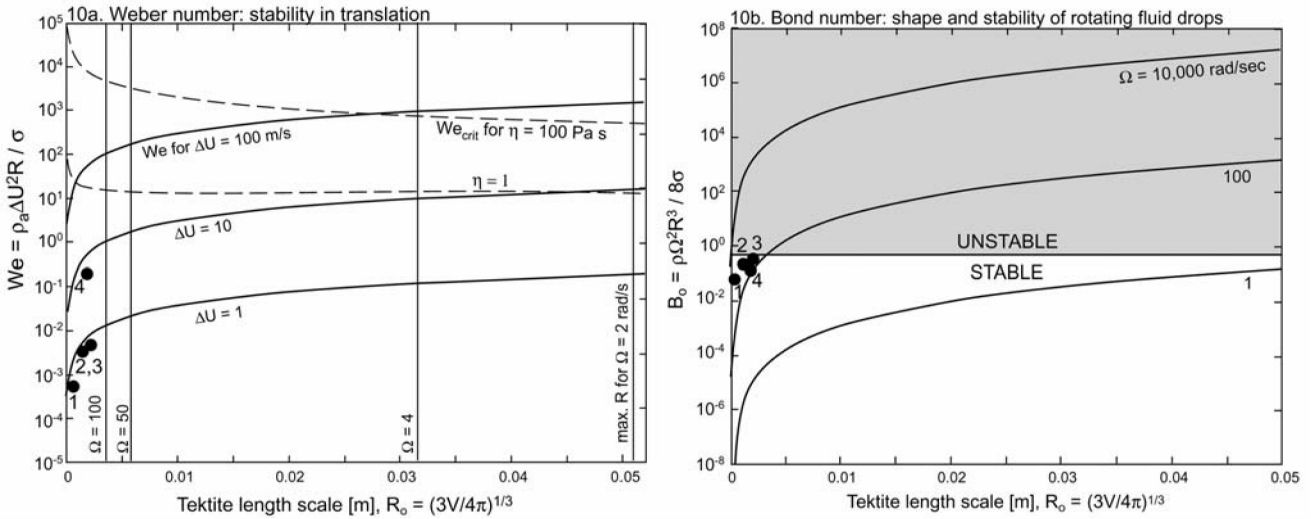
Fig. 10. The stability characteristics of natural and laboratory tektites: a) the Weber number, indicating the stability of translating drops, is shown as a function of length scale (R) over a range of relative velocities (ΔU). The critical Weber number, Equation 9, below which breakup does not occur, is shown as a function of viscosity in dashed curves. Note that the critical Weber number depends on (R) through the Ohnesorge number. In pure translation, tektites below their critical Weber number are stable. Viscosities as low as 100 Pa s allow translating tektites as large as 0.05 m to exist even at $\Delta U > 100$ m/s. Rotation-induced instability, however, prevents large tektites from forming as equilibrium bodies. When rotation is included, the maximum radii for various rotational velocities are shown in the vertical lines, calculated from Equation 15. For a tektite traveling at a differential velocity below its terminal velocity and rotating at 1 rad/s, the maximum radius is 0.08 m. These curves, and those of (b), are calculated using the physical parameters in Table 1. The experiments illustrated in Figs. 4, 5, 7, and 8 are shown as filled circles 1–4; b) the Bond number, indicating the equilibrium shape of a rotating fluid drop, is plotted as a function of tektite length scale (R) for varying rotational velocity (Ω) using the physical parameters from Table 1. Drops with $B_o > 0.57$ are destabilized by rotation. All but the smallest and most slowly rotating natural tektites are unstable and prone to breakup induced by rotation. While cm-sized tektites in pure translation are stable to breakup at low ΔU, rotating centimetric tektites are disequilibrium forms and can only be stabilized by high viscosity. The experiments illustrated in Figs. 4, 5, 7, and 8 are shown as filled circles 1–4.

and tumbling drops. In particular, the toroidal forms found to be metastable for rolling drops are unstable for an equivalent tumbling motion, where dumbbell forms are preferred.

Scaling arguments describing the dynamics and form of tumbling fluid bodies yield a simple criterion (Equation 11) for such bodies to take the form of bodies of revolution: their rotational speed must be at least 1% of their translational speed. In the case of tektites, the prevalence of bodies of revolution clearly results from the density difference between the tektite fluid and air. We have summarized scaling arguments describing the breakup of droplets in flight that govern the size range of tektites. We focused on the case of isothermal drops with constant fluid properties to obtain predictions (specifically Equations 7 and 15) for the maximum sustainable size of a drop of molten tektite fluid. The bounds on tektite drop sizes so obtained are weak owing to the large uncertainties in both the relative velocity between the tektite and ambient and the physical properties of the tektite fluid, especially the fluid viscosity. Choosing the terminal speed as ΔU suggests that the largest stable equilibrium rotating tektite is approximately 3 mm and that all cm-sized natural tektites are, thus, the product of cooling and quenching before breakup (e.g., Matsuda et al. 1996). Another possibility is that the relative speed between the tektites and ambient before solidification was substantially

less than the terminal speed. We note that a number of tektites corresponding to bodies of rotation have been observed to have a relatively high viscosity crust that evidently cracked during flight (O'Keefe 1976).

Our study underscores the importance of the in-flight cooling and quenching of tektite fluid. The thermodynamic and fluid dynamical considerations arising in the problem of cooling, tumbling drops in flight will be treated elsewhere. Particular attention will be given to making estimates for the relative magnitudes of the drop cooling time, flight time, and droplet breakup time. The resulting heat transfer problem requires consideration of convective, diffusive, and radiative heat transport from the tektite in addition to dissipative heating in the boundary layers surrounding the tumbling tektite body.

Finally, we note that the correspondence of the form of splash-form tektites to bodies of revolution does not necessarily imply that the tektites were splashed off the ground in fluid form. The possibility that some tektites are the products of condensation from a vapor phase (Melosh 1990; Margolis et al. 1991), in which case they would fall to earth in the form of tektite rain or hail, will be the subject of future consideration.

Editorial Handling—Dr. Alex Deutsch

REFERENCES

Adams E. W. and Huffaker R. M. 1962. Application of ablation analysis to the tektite problem. *Journal of Geophysical Research* 67:3537.

Adams E. W. and Huffaker R. M 1964. Aerodynamic analysis of the tektite problem. *Geochimica et Cosmochimica Acta* 28:881–892.

Albin E. F, Norman M. D., and Roden M. 2000. Major and trace element compositions of georgianites: Clues to the source of North American tektites. *Meteoritics* 35:795–806.

Aussillous P. and Quéré D. 2001. Liquid marbles. *Nature* 411:924–927.

Barnes V. E. 1990. Tektite research 1936–1990. *Meteoritics* 25:149–159.

Barnes V. E. and Barnes M. A. 1973. *Tektites.* Stroudsberg: Dowden, Hutchison, and Ross Inc. 445 p.

Beyer H. O. 1962. *Philippine Tektites, Vol. 1 Part 2.* Manila: University of The Philippines. 290 p.

Bottinga Y. and Weil D. F. 1972. The viscosity of magmatic silicate liquids: A model for calculation. *American Journal of Science* 272:438–475.

Brodkey R. S. 1969. *The phenomena of fluid motions.* Reading: Addison-Wesley. 737 p.

Brown R. A. and Scriven L. E. 1980. The shape and stability of rotating liquid drops. *Proceedings of the Royal Society of London Series A* 371:331–357.

Chandrasekhar S. 1965. The stability of a rotating liquid drop. *Proceedings of the Royal Society of London Series A* 286:1–26.

Clift R., Grace J. R., and Weber M. E. 1978. *Bubbles, drops, and particles.* New York: Academic Press. 380 p.

Eggers J. 1997. Nonlinear dynamics and breakup of free surface flows. *Reviews of Modern Physics* 69:865.

Dingwell D. B., Hess K. U., and Romano C. 2000. Viscosities of granitic (sensu lato) melts: Influence of the anorthite component. *American Mineralogist* 85:1342–1348.

Frey F. A. 1977. Microtektites: A chemical comparison of bottle-green microtektites, normal microtektites, and tektites. *Earth and Planetary Science Letters* 35:43–48.

Glass B. P. 1972. Bottle green microtektites. *Journal of Geophysical Research* 77:7057.

Hsiang L. P. and Faeth G. M. 1992. Near-limit drop deformation and secondary breakup. *International Journal of Multiphase Flow* 18:635–652.

King E. A. 1977. The origin of tektites: A brief review. *American Scientist* 65:212–218.

Klein L. C., Yinnon H., and Uhlmann D. R. 1980. Viscous flow and crystallization behavior of tektite glasses. *Journal of Geophysical Research* 85:5485–5489.

Koeberl C. 1990. The geochemistry of tektites: An overview. *Tectonophysics* 171:405–422.

Mahadevan L. and Pomeau Y. 1999. Rolling droplets. *Physics of Fluids* 11:2449–2453.

Margolis S.V., Claeys P., and Kyte F. T. 1991. Microtektites, microkrystites, and spinels from a late Pliocene asteroid impact in the Southern ocean. *Science* 251:1594–1597.

Matsuda J. I., Mariuoka T., Pinti D. L., and Koeberl, C. 1996. Noble gas study of a phillippinite with an unusually large bubble. *Meteoritics* 31:273–277.

McColl D. H. 1997. A flanged toroidal tektite from Australia. *Meteoritics* 32:981–982.

Meisel T., Lange J. M., and Krähenbühl U. 1997. The chemical variation of moldavite tektites: Simple mixing of terrestrial sediments. *Meteoritics* 32:493–502.

Melosh H. J. 1998. Impact physics constraints on the origin of tektites. *Meteoritics* 33:A104.

Melosh H. J. 1990. Vapour plumes: A neglected aspect of impact cratering. *Meteoritics* 25:386.

Melosh H. J. and Vickery A. M. 1991. Melt droplet formation in energetic impact events. *Nature* 350:494–497.

O'Keefe J. A. 1976. *Tektites and their origin.* New York: Elsevier Press. 254 p.

Palme H. and Larimer J. W. 1988. Moderately volatile elements. In *Meteorites and the early solar system.* Tucson: University of Arizona Press. pp. 436–461.

Pilch M. and Erdman C. A. 1987. Use of breakup time data and velocity history data to predict the maximum size of stable fragments for acceleration-induced breakup of a liquid drop. *International Journal of Multiphase Flow* 13:741–757.

Plateau J. A. F. 1863. Experimental and theoretical researches on the figures of equilibrium of a liquid mass withdrawn from the action of gravity. Annual Report of the Board of Regents of the Smithsonian Institution, Washington, D.C. pp. 270–285.

Reinhart J. S. 1958. Impact effects and tektites. *Geochimica et Cosmochimica Acta* 14:287–290.

Richard D. and Quéré D. 1999. Viscous drops rolling on a tilted non-wettable solid. *Europhysics Letters* 48:286–291.

Riley G. N., Jr. and Kohlstedt D. L. 1991. Kinetics of melt migration in upper mantle-type rocks. *Earth and Planetary Science Letters* 105:500–521.

Shaw H. R. 1972. Viscosities of magmatic silicate liquids: An empirical method of prediction. *American Journal of Science* 272:870–893.

Stanley V., Barnes V., Cloud P., and Fisher R. V. 1971. Surface micrography of lunar fines compared with tektites and terrestrial volcanic analogs. Proceedings, 2nd Lunar and Planetary Science Conference. pp. 909–921.

Steel D. 1998. Distributions and moments of asteroid and comet impact speeds upon the earth and Mars. *Planetary and Space Science* 46:473–478.

Stöffler D., Artemieva N.A., and Pierazzo E. 2002. Modeling the Ries-Steinheim impact event and the formation of the Moldavite strewn field. *Meteoritics* 37:1893–1908.

Taylor S. R. 1973. Tektites: A post-Apollo view. *Earth Science Reviews* 9:101–123.

Walcott R. H. 1898. The occurrence of so-called obsidian bombs in Australia. *Proceedings of the Royal Society of Victoria* 11:23–53.